IEEE Access
Multidisciplinary | Rapid Review | Open Access Journal

Date of publication xxxx 00, 0000, date of current version xxxx 00, 0000.

Digital Object Identifier 10.1109/ACCESS.2019.DOI

Real-Valued Orthogonal Sequences for Iterative Channel Estimation in MIMO-FBMC Systems

JING ZHANG[1], SU HU[1], ZILONG LIU[2], PEI WANG[1], PEI XIAO[2], YUAN GAO[3,4]

[1]National Key Laboratory on Communications, University of Electronic Science and Technology of China, Chengdu, 611731, China
[2]Institute of Communication Systems, 5G Innovation Centre, University of Surrey, GU2 7XH, United Kingdom
[3]Academy of Military Science of PLA, Beijing, 100091, China
[4]Department of Electronic Engineering, Tsinghua University, Beijing, 100084, China

Corresponding author: SU HU (husu@uestc.edu.cn), YUAN GAO (yuangao08@tsinghua.edu.cn).

The authors would like to thank the anonymous reviewers for their valuable comments. This work is jointly supported by MOST Program of International S&T Cooperation (No.2016YFE0123200), National Natural Science Foundation of China (No. 61701503/61750110527), and National Key R&D Program of China (No.2018YFC0807101).

ABSTRACT In this paper, we present a novel sequence design for efficient channel estimation in multiple input multiple output filterbank multicarrier (MIMO-FBMC) system with offset QAM modulation. Our proposed sequences, transmitted over one FBMC/OQAM symbol, are real-valued in the frequency domain and display zero-correlation zone properties in the time-domain. The latter property enables optimal channel estimation for a least-square estimator in frequency-selective fading channels. To further improve the system performance, we mitigate the data interference by an iterative feedback loop between channel estimation and FBMC demodulation. Simulation results validate that our proposed real-valued orthogonal sequences and the iterative channel estimation and demodulation scheme provide a practical solution for enhanced performance in preamble-based MIMO-FBMC systems.

INDEX TERMS MIMO-FBMC, channel estimation, preamble, real-valued orthogonality, zero-correlation zone sequences, feedback iteration loop.

I. INTRODUCTION

Filterbank multicarrier systems employing offset quadrature amplitude modulation (OQAM [1]), called FBMC/OQAM or FBMC, have attracted significant research attention in recent years [2], [3]. From here on, we shall use FBMC to denote "FBMC/OQAM", although there exist other FBMC variants too. As known, orthogonal frequency division multiplexing (OFDM) system has disadvantages of low spectral efficiency (because of the cyclic prefix), sensitivity to frequency deviation and high peak-to-average power ratio. An FBMC system achieves higher spectrum efficiency without the need of cyclic prefix (CP), compared to OFDM. Each FBMC system is equipped with a properly designed pulse shaping filter having good time-frequency localization property. Benefiting from this, an FBMC system has very low out-of-band power leakage and enhanced robustness against time/frequency synchronization errors (e.g., carrier frequency offset).

In contrast to the "complex-field orthogonality" in CP-OFDM systems, the subcarrier functions in FBMC are orthogonal in the real field only. This results in the intrinsic imaginary interference incurred from adjacent symbols [4], [5], making channel estimation more challenging than that in CP-OFDM systems. A series of training schemes and associated estimation methods for preamble-based FBMC systems have been discussed in [4]–[9]. The interference approximation method (IAM), which is capable of computing an approximation of the interference from neighboring training symbols, has been proposed to improve the estimation performance [6]–[9]. Another representative approach to cope with the intrinsic imaginary interference is called interference cancellation method (ICM) [10], [11]. In ICM pilot structure, by properly setting the value of the surrounding pilots, the data interference of the symmetrical position around the pilot frequency can be made very small. Recently, a simple time-domain channel estimation approach, which has no specific requirement for the length of the symbol interval (compared to the maximum channel delay spread), has been proposed in

[12].

In addition to the intrinsic imaginary interference, the multi-antenna interference elimination in channel estimations is also a challenging problem for MIMO-FBMC [13]–[17]. It is noted that the channel estimations in MIMO systems are more complicated than that in single input single output (SISO) systems as more channel fading coefficients need to be measured [18]. A naive training scheme for MIMO-FBMC is that the preambles from different antennas are placed over different symbols separated by guard intervals. But this is highly inefficient as a large amount of training overhead could be incurred [15]–[16].

In multipath fading channels, zero-correlation zone (ZCZ) sequences may be employed as training sequences in MIMO systems to achieve optimal channel estimation provided that all the arrival signals are quasi-synchronous within a window [19]–[22]. Only when the time delay of the channel is less than the length of ZCZ, the sequences on different antennas can remain orthogonal. However, ZCZ sequences rely on correlation in the complex-domain, which may not be obtained in FBMC systems with the real-field orthogonality only. To circumvent this problem, a training method called complex training sequence decomposition (CTSD) has been developed by us in [23]. CTSD purposely splits the real- and imaginary- parts of the frequency domain duals of ZCZ sequences and then sends them over two separate training symbols, based on code division multiplexing (CDM) [23]–[31]. The primary objective of this paper is to improve the CTSD for enhanced channel estimation efficiency with only one non-zero FBMC preamble.

The contributions of this paper are twofold: Firstly, we propose real-valued sequences which can be applied as non-zero frequency-domain preambles in MIMO-FBMC systems. These preamble sequences display ZCZ property in the time-domain and lead to minimum mean-squared error (MSE) under least square estimator [32]–[35]. Secondly, we propose an iterative feedback receiver structure which carries out recursive interference mitigation between channel estimation and data demodulation to further eliminate system interference.

The paper is organized as follows: Section II presents the system model of FBMC system and introduces existing preamble-based channel estimation methods. In Section III, we present a design of training symbols method with real-valued orthogonality and capability of interference self-cancellation, followed by detailed description of corresponding feedback iteration estimation scheme for interference elimination. In addition, numerical simulations are discussed in Section IV. Finally, this paper is summarized in Section V.

II. SYSTEM MODEL AND PROBLEM FORMULATION

A. SYSTEM MODEL OF MIMO-FBMC SYSTEMS

Considering an FBMC baseband model with M subcarriers, the equivalent discrete-time sending FBMC signal can be defined as [36]

$$s(l)=\sum_{n\in Z}\sum_{m=0}^{M-1}a_{m,n}\underbrace{j^{m+n}e^{j2\pi ml/M}g\left(l-n\frac{M}{2}\right)}_{g_{m,n}(l)}, \quad (1)$$

where $j=\sqrt{-1}$ and $a_{m,n}$ is the real-valued OQAM symbol transmitted over the m-th subcarrier and the n-th time-slot. The length of an FBMC/OQAM symbol is half of an OFDM symbol. Meanwhile, $g\left(l\right)$ is the impulse response of symmetrical real-valued prototype filter with length of $L_g=KM$ and K is the overlapping factor. $g_{m,n}(l)$ represents the synthesis basis which is obtained by the time-frequency translated version of $g\left(l\right)$, where the transmultiplexer response of $g_{m,n}(l)$ is defined as

$$\zeta_{m,n}^{p,q}=\sum_{l=-\infty}^{\infty}g_{m,n}(l)g_{p,q}^{*}(l). \quad (2)$$

TABLE 1: Transmultiplexer response of PHYDYAS filter [37]

	$n-2$	$n-1$	n	$n+1$	$n+2$
$m-2$	-0.0001	0	0	0	-0.0001
$m-1$	$0.125j$	$-0.2058j$	$0.2393j$	$-0.2058j$	$0.125j$
m	-0.0002	$0.5644j$	$\mathbf{1}$	$-0.5644j$	-0.0002
$m+1$	$-0.125j$	$-0.2058j$	$-0.2393j$	$-0.2058j$	$-0.125j$
$m+2$	-0.0001	0	0	0	-0.0001

In this paper, we employ the pulse shaping filter of PHYDYAS project, where the transmultiplexer response is shown in Table 1. It is noted that all the values of interference are purely imaginary, except at $(m,n)=(p,q)$. This is due to the fact that FBMC systems only satisfy the real-field orthogonality, meaning that perfect reconstruction of real-valued symbol $a_{m,n}$ is obtained if and only if the following orthogonality condition is held [36]:

$$\Re\left\{\sum_{l=-\infty}^{\infty}g_{m,n}(l)g_{p,q}^{*}(l)\right\}=\delta_{m,p}\delta_{n,q}, \quad (3)$$

where $\delta_{m,p}$ is the Kronecker delta function, which is equal to 1 if and only if $m=p$. On the other hand, there will be intrinsic imaginary interference for any lattice point $(m,n)\neq(p,q)$, even passing through a distortion-free channel.

Let $\mathbf{h}=\left[h\left(0\right),h\left(1\right),\cdots,h\left(L_h-1\right)\right]^T$ be the discrete impulse response of a multipath fading channel, where L_h denotes the time domain tap coefficients number of the channel. According to (1), the baseband received signal can be written as

$$r\left(l\right)=\sum_{\tau=0}^{L_h-1}h\left(\tau\right)s\left(l-\tau\right)+\eta\left(l\right), \quad (4)$$

where $\eta\left(l\right)$ denotes the complex additive white gaussian noise with zero mean and variance of σ^2. The demodulation of received signal at the (m,n)-th time-frequency lattice

point provides a complex symbol given as

$$y_{m,n} = \sum_{l=-\infty}^{\infty} r\left(l\right) j^{m+n} g\left(l - \frac{nM}{2}\right) e^{-j2\pi ml/M}. \quad (5)$$

Assuming that the maximum channel delay spread $\tau_{\max}$ is much shorter than the symbol interval, i.e., $\tau_{\max} \ll T$. Therefore, the channel may be viewed as frequency flat at each subcarrier over the prototype filter over any time interval of $[l, l+\tau_{\max}]$, i.e., $g\left(l\right) \approx g\left(l+\tau\right)$, for $\tau \in [0, \tau_{\max}]$. Hence, regardless of the delay and combining the above formulas, $y_{m,n}$ in (5) can be expressed in terms of $a_{m,n}$, $\zeta_{m,n}^{p,q}$ in the following form [38]

$$y_{m,n} = H_{m,n}a_{m,n} + \underbrace{\sum_{(p,q)\neq(m,n)} H_{p,q}a_{p,q}\zeta_{m,n}^{p,q}}_{I_{m,n}} + \eta_{m,n}, \quad (6)$$

where $H_{m,n}$ denotes the channel frequency response at the (m,n)-th lattice point, and $I_{m,n}$ and $\eta_{m,n}$ are the intrinsic interference and noise terms, respectively.

The above FBMC formulation in SISO scenario may be easily extended to MIMO-FBMC systems. Consider an $N_T \times N_R$ MIMO-FBMC system, the received signal in each receiving antenna $k = 1, 2, \cdots, N_R$ can be expressed as

$$y_{m,n}^{k} = \sum_{i=1}^{N_T} \left(H_{m,n}^{k,i} a_{m,n}^{i} + \sum_{\substack{(m,n) \\ \neq(p,q)}} H_{p,q}^{k.i} a_{p,q}^{i} \zeta_{m,n}^{p,q} \right) + \eta_{m,n}^{k}, \quad (7)$$

where $H_{m,n}^{k,i}$ denotes the channel frequency response from the i-th transmitting antenna to the k-th receiving antenna, and $\eta_{m,n}^{k}$ denotes the corresponding noise component in the k-th receiving antenna.

B. OVERVIEW OF TRADITIONAL METHODS

To eliminate interference between antennas as much as possible, a simple preamble structure for MIMO-FBMC, shown in Fig. 1, can be obtained by transmitting training symbols (separated by G columns of zeros) over different antennas in different time-slots. For a MIMO-FBMC system with N_T transmitting antennas, this training structure requires $(G+1)N_T$ real-valued training symbols when G columns zero symbols (for every two adjacent antennas) are inserted. Clearly, there could be huge waste of time-frequency resources for large N_T.

Since it is a waste of spectrum resources to place preambles from different antennas by time-division method, CTSD has been proposed to reduce the training overhead by reconstructing the complex-field orthogonality of MIMO-FBMC signals [23]. Preambles of different antennas are placed on the same time slot by means of CDM. As shown in Fig. 2, the real and imaginary parts of the frequency domain of a complex ZCZ preamble sequence are respectively put into two different FBMC symbols separated by zeros. Although significant training overhead has been saved by CTSD, it still requires $3G$+2 real-valued training symbols.

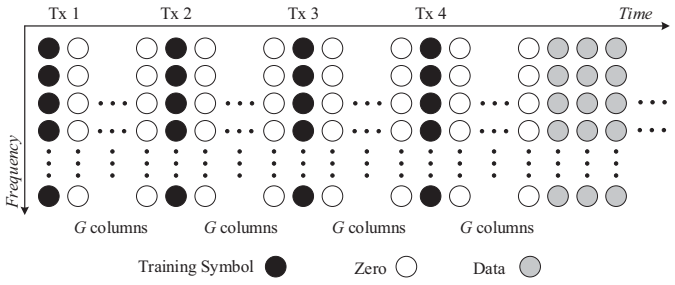

FIGURE 1: Conventional preamble for 4×4 MIMO-FBMC systems with G zero symbols for every two adjacent antennas [39].

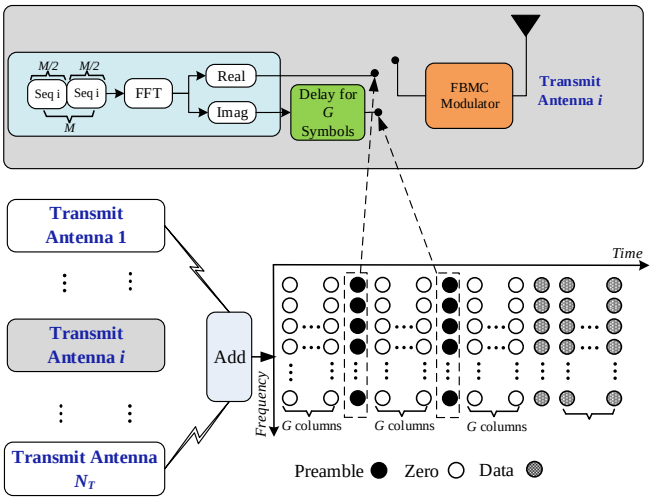

FIGURE 2: The preamble structure of CTSD in [23].

III. EFFICIENT PREAMBLE CHANNEL ESTIMATION

A. PREAMBLE DESIGN OF REAL-VALUED ORTHOGONAL SEQUENCES

Let $\mathbf{A} = \{\mathbf{a}_1, \mathbf{a}_2, \cdots, \mathbf{a}_{N_T}\}$ be a sequence set of N_T sequences, each having length M, i.e.,

$$\mathbf{a}_i = [a_i(0), a_i(1), \cdots, a_i(M-1)]^T, \quad (8)$$

where M is the total number of subcarriers. The corresponding frequency-domain training sequences $\{\mathcal{A}_1, \mathcal{A}_2, \cdots \mathcal{A}_{N_T}\}$ can be shown as

$$\begin{aligned} \mathcal{A}_i &= [A_i(0), A_i(1), \cdots A_i(M-1)]^T, \\ A_i(m) &= \frac{1}{\sqrt{M}} \sum_{n=0}^{M-1} a_i(n) e^{\frac{-j2\pi mn}{M}}, 0 \leq m \leq M-1. \end{aligned} \quad (9)$$

The following conditions should be satisfied when designing training sequence set $\mathbf{A} = \{\mathbf{a}_1, \mathbf{a}_2, \cdots, \mathbf{a}_{N_T}\}$.

1) All the frequency-domain training sequences $\mathcal{A}_i$ are real-valued and $A_i(m) = 0$ for all the odd m;

2) Under linear least square channel estimator, it has been proved in [23] that the channel estimation minimum MSE (MMSE) can be achieved if and only if the following

condition is held:

$$\begin{bmatrix} \mathbf{S}_1^H\mathbf{S}_1 & \mathbf{S}_2^H\mathbf{S}_1 & \cdots & \mathbf{S}_{N_T}^H\mathbf{S}_1 \\ \mathbf{S}_1^H\mathbf{S}_2 & \mathbf{S}_2^H\mathbf{S}_2 & \cdots & \mathbf{S}_{N_T}^H\mathbf{S}_2 \\ \vdots & \vdots & \ddots & \vdots \\ \mathbf{S}_1^H\mathbf{S}_{N_T} & \mathbf{S}_2^H\mathbf{S}_{N_T} & \cdots & \mathbf{S}_{N_T}^H\mathbf{S}_{N_T} \end{bmatrix} = M\mathbf{I}_{N_T L_h}, \tag{10}$$

with

$$\mathbf{S}_i = \begin{bmatrix} a_i(0) & a_i(M-1) & \cdots & a_i(M-L_h+1) \\ a_i(1) & a_i(0) & \cdots & a_i(M-L_h+2) \\ \vdots & \vdots & \ddots & \vdots \\ a_i(M-1) & a_i(M-2) & \cdots & a_i(M-L_h) \end{bmatrix}. \tag{11}$$

It is clear that sequences in $\mathcal{A}$ should have zero periodic auto- and cross- correlation properties for time-shifts not exceeding L_h from above two formulas. Note that real-valued $\mathcal{A}_i$ is for training overhead reduction, whereas $A_i(m) = 0$ for all the odd m is set for ICI (inter-carrier interference) suppression.

Denote $\left[\mathbf{S}_{i_1}^H\mathbf{S}_{i_2}\right]_{t_1,t_2}$ for the (t_1,t_2) element of the submatrix $\mathbf{S}_{i_1}^H\mathbf{S}_{i_2}$ in (10). Observe that each column of $\mathbf{S}_i$ is a cyclically-shifted version of $\mathbf{a}_i$. By applying the inverse discrete Fourier transform (IDFT) to $\mathbf{a}_{i_1}$, $\mathbf{a}_{i_2}$, and keeping in mind that $\mathcal{A}_i$ should be real-valued, we have $\left[\mathbf{S}_{i_1}^H\mathbf{S}_{i_2}\right]_{t_1,t_2}$ can be represented as

$$\begin{aligned} &\left[\mathbf{S}_{i_1}^H\mathbf{S}_{i_2}\right]_{t_1,t_2} \\ &= \sum_{t=0}^{M-1} a_{i_1}^*(t-t_1+1)a_{i_2}(t-t_2+1) \\ &= \tfrac{1}{M^2}\sum_{m_1,m_2=0}^{M-1} A_{i_1}(m_1)A_{i_2}(m_2)W_M^{(t_1-1)m_1-(t_2-1)m_2} \\ &\qquad \cdot \sum_{t=0} W_M^{t(m_2-m_1)} \\ &= \tfrac{1}{M}\sum_{m=0}^{M-1} A_{i_1}(m)A_{i_2}(m)W_M^{(t_1-t_2)m}, \end{aligned} \tag{12}$$

where $W_M = e^{\frac{-j2\pi}{M}}$. In particular, when $i_1 = i_2$, the equation can be reduced to

$$\left[\mathbf{S}_{i_1}^H\mathbf{S}_{i_2}\right]_{t_1,t_2} = \frac{1}{M}\sum_{m=0}^{M-1} A_{i_1}^2(m)W_M^{(t_1-t_2)m}. \tag{13}$$

Let $L = M/N_T$ and consider a binary sequence $\mathbf{B} = [B_0, B_1, \cdots, B_{L-1}]$ over $\{1,-1\}$. Frequency-domain training sequences $\{\mathcal{A}_0, \mathcal{A}_1, \cdots \mathcal{A}_{N_T-1}\}$ are defined as follows:

$$A_i(m) = \begin{cases} \sqrt{N_T}(-1)^{ip}B_p, & m/2 = \lfloor i/2 \rfloor + p(N_T/2), \\ 0, & \text{otherwise}, \end{cases} \tag{14}$$

where $i \in \{0,1,\cdots,N_T-1\}$ and $m \in \{0,1,\cdots,M-1\}$.

Example 1: Let $L = 4$ and $N_T = 4$. Hence, $M = N_T L = 16$. $[\mathcal{A}_1, \mathcal{A}_2, \mathcal{A}_3, \mathcal{A}_4]^T$ can be expressed in the following matrix

$$\begin{bmatrix} B_0,0,0,0,B_1,0,0,0,B_2,0,0,0,B_3,0,0,0 \\ \bar{B}_0,0,0,0,\bar{B}_1,0,0,0,\bar{B}_2,0,0,0,\bar{B}_3,0,0,0 \\ 0,0,B_0,0,0,0,B_1,0,0,0,B_2,0,0,0,B_3,0 \\ 0,0,\bar{B}_0,0,0,0,\bar{B}_1,0,0,0,\bar{B}_2,0,0,0,\bar{B}_3,0 \end{bmatrix}, \tag{15}$$

where $\bar{B}_p$ denotes for $-B_p$. Next, we proceed with the discussion for the following two cases:

1) When $i_1 \neq i_2$. We deal with the case for "even i_1 and $i_2 = i_1 + 1$". In this case, the positions of all the non-zero entries in $\mathcal{A}_{i_1}$ are identical to those of $\mathcal{A}_{i_2}$. Let $m = i_1 + pN_T$, then (10) is reduced to

$$\begin{aligned} &\left[\mathbf{S}_{\text{even } i_1}^H\mathbf{S}_{i_2=i_1+1}\right]_{t_1,t_2} \\ &= \tfrac{1}{M}\sum_{m=0}^{M-1} A_{i_1}(m)A_{i_1+1}(m)W_M^{(t_1-t_2)m} \\ &= \tfrac{1}{M}\sum_{p=0}^{L-1}(-1)^{i_1p+(i_1+1)p}B_p^2W_M^{(t_1-t_2)(i_1+pN_T)} \\ &= \tfrac{W_M^{(t_1-t_2)i_1}}{M}\cdot\sum_{p=0}^{L-1}(-1)^pW_L^{(t_1-t_2)p}. \end{aligned} \tag{16}$$

It can be easily shown that

$$\sum_{p=0}^{L-1}(-1)^pW_L^{(t_1-t_2)p} = 0, \tag{17}$$

provided that L is an even number not less than 4 and $|t_1 - t_2| \neq L/2$.

For the case of $i_1 \neq i_2$, the position set of all the non-zero entries in $\mathcal{A}_{i_1}$ is disjoint with that of $\mathcal{A}_{i_2}$. This implies that $A_{i_1}(m)A_{i_2}(m) = 0$ for all $m \in \{0,1,\cdots,M-1\}$. Consequently, $\left[\mathbf{S}_{i_1}^H\mathbf{S}_{i_2}\right]_{t_1,t_2} = 0$ for any t_1, t_2.

2) When $i_1 = i_2$. By (13) and (14), $\left[\mathbf{S}_{i_1}^H\mathbf{S}_{i_2}\right]_{t_1,t_2}$ can be rewritten as

$$\begin{aligned} \left[\mathbf{S}_{i_1}^H\mathbf{S}_{i_2}\right]_{t_1,t_2} &= \frac{1}{M}\sum_{m=0}^{M-1} W_M^{(t_1-t_2)m} \\ &= \frac{W_M^{(t_1-t_2)2\lfloor i_1/2 \rfloor}}{M}\cdot\sum_{p=0}^{L-1}W_L^{(t_1-t_2)p} \\ &= 0, \end{aligned} \tag{18}$$

provided that $(t_1 - t_2) \bmod L \neq 0$.

Based on the analysis for the above two cases, it is quite clear that $\mathbf{A}$ obtained through IDFT from the frequency-domain sequences $[\mathcal{A}_0, \mathcal{A}_1, \mathcal{A}_2, \mathcal{A}_{N_T-1}]^T$ in (14), is a valid training sequence set for $L_h \leq L/2$, where L should be an even number not less than 4.

B. EFFICIENT CHANNEL ESTIMATION FOR MIMO-FBMC SYSTEMS

The N_T sequences designed in the preceding subsection can be simultaneously transmitted over N_T transmitting antennas. According to Table I, both ISI and ICI received at the (m,n)-th time-frequency lattice point are mainly from the nearest neighboring lattices, whereas the interference from other lattices is negligible. As shown in Fig. 3, the

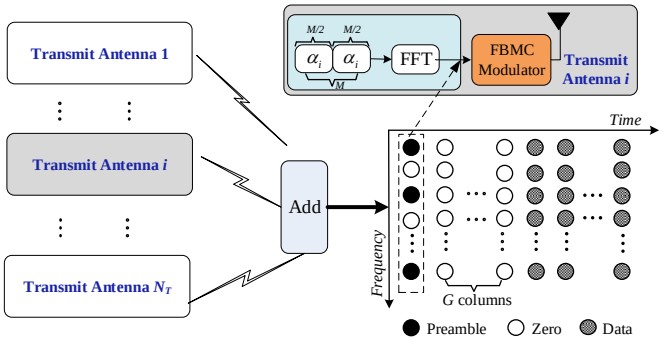

FIGURE 3: Channel estimation of the kth receive antenna of MIMO-FBMC system.

proposed real-valued orthogonal sequences suppress ISI by inserting G columns of zero symbols nearby the (m,n)-th time-frequency. Furthermore, for even $m=k$, ICI is mainly from the $(m\pm1,n)$ lattice points which have zero values. Because of this, ICI can be substantially suppressed by the proposed method. In addition, the real-valued orthogonal sequences take up only an FBMC symbol and 3 columns of zeros, which reduces the training overhead.

For a $N_T\times N_R$ MIMO-FBMC system, there are N_TN_R independent channels to be measured, in which each channel is modelled as a finite impulse response filter with L_h taps. For ease of analysis, assumed that $N_T=N_R$ and the system is quasi-static. The channel impulse response can be denoted as [23]

$$\mathbf{h}_{i,k}=[h_{i,k}(0),h_{i,k}(1),\cdots,h_{i,k}(L-1)]^T, \tag{19}$$

where $\mathbf{h}_{i,k}$ represents the channel impulse response vector from the i-th $(i=1,2,\cdots,N_T)$ transmitting antenna to the k-th $(k=1,2,\cdots,N_R)$ receiving antenna. Similar to SISO-FBMC system, the demodulation of the received signal at the (m,n)-th lattice point in the k-th receiving antenna can be written as

$$y_k(m,n)\approx\sum_{i=1}^{N_T}\sum_{\tau=0}^{L_h-1}\sum_{\substack{p=0\\q\in Z}}^{M-1}a_{p,q}^{i}\zeta_{m,n}^{p,q}\times W_M^{p\tau}h_{i,k}(\tau)+\eta_k(m,n). \tag{20}$$

The received symbol $\mathbf{y}_k=[y_k(0),y_k(1),\cdots,y_k(M-1)]^T$ associated to $\mathcal{A}_i$ can be expressed as

$$y_k(m)\approx\sum_{i=1}^{N_T}\sum_{\tau=0}^{L_h-1}A_i(m)e^{-j2\pi m\tau/M}h_{i,k}(\tau)+\eta_k(m)\ . \tag{21}$$

Note that $A_i(m)=\sum_{n=0}^{M-1}a_i(n)W_M^{m,n}$, and $(\cdot)_M$ represents the modulo M operation. Let $n'=n+\tau$, then $y_k(m)$ can be simplified to

$$y_k(m)=\sum_{\tau=0}^{L_h-1}\left(\sum_{i=1}^{N_T}\left(\sum_{n'=0}^{M-1}a_i(n'-\tau)_MW_M^{mn'}\right)h_{i,k}(\tau)\right)+\eta_k(m)\ . \tag{22}$$

Applying IFFT to $\mathbf{y}_k$, the received signal can be demodulated to $\mathbf{r}_k$

$$\mathbf{r}_k=\sum_{\tau=0}^{L_h-1}\left(\sum_{i=1}^{N_T}a_i(n'-\tau)_Mh_{i,k}(\tau)\right)+\omega_k(m)\ . \tag{23}$$

The equation (23) can be written in matrix form as $\mathbf{r}_k=\mathbf{S}\mathbf{h}_k+\boldsymbol{\omega}_k$, where $\mathbf{S}=[\mathbf{S}_1,\mathbf{S}_2,\cdots,\mathbf{S}_{N_T}]^T$ and $\mathbf{S}_i$ has been represented as (11).

$$\begin{aligned}\boldsymbol{\omega}_k&=[\omega_k(0),\omega_k(1),\cdots,\omega_k(M-1)]^T,\\ \omega_k(n)&=\frac{1}{M}\sum_{m=0}^{M-1}\eta_k(m)e^{j2\pi mn/M}.\end{aligned} \tag{24}$$

Since the rank of $\mathbf{S}$ is equal to the number of columns for $M>L_h$, the linear least square channel estimator for the k-th receiving antenna can be written as

$$\tilde{\mathbf{h}}_k=[\tilde{h}_{1,k},\tilde{h}_{2,k},\cdots,\tilde{h}_{N_T,k}]^T=(\mathbf{S}^H\mathbf{S})\mathbf{S}^H\mathbf{r}_k\ . \tag{25}$$

If the noise terms satisfy zero-mean white normal distribution, it is evident that the channel estimator is unbiased, i.e., $\mathbb{E}[\tilde{\mathbf{h}}_k]=\mathbf{h}_k$. Thus, the channel estimation MSE can be expressed as

$$\mathrm{MSE}=\mathbb{E}\left[(\mathbf{h}_k-\tilde{\mathbf{h}}_k)^H(\mathbf{h}_k-\tilde{\mathbf{h}}_k)\right]=2\sigma^2\mathrm{Tr}((\mathbf{S}^H\mathbf{S})^{-1}), \tag{26}$$

where $\mathbb{E}(\cdot)$ denotes the expectation and $\mathrm{Tr}(\cdot)$ denotes the matrix trace operation.

IV. ITERATIVE RECEIVER STRUCTURE FOR INTERFERENCE MITIGATION

Our proposed sequence design is to satisfy the requirement of FBMC systems for purely real-valued preambles, whereas the pilot transmission structure is to meet the constraint condition of preamble cross-correlation condition for mitigation of inter-antenna interference. Although G columns of zeros have been inserted between preamble and data symbols and set even subcarriers to zero, there may still exist inevitable data interference. As a result, the internal interference may lead to degraded channel estimation.

As an example, let us consider $G=1$ and analyze the data interference under the proposed pilot transmission structure. In this case, the even subcarriers are set to zeros and a column of zero separates the pilot from data, as shown in Fig. 4. Thus, only the interference from first data symbol needs to be considered. For the target pilot shown in Fig. 4, the total residual interference from surrounding data is $|\varepsilon+2\beta+2j\gamma|$, where $\varepsilon=0.0002,\beta=0.001,\gamma=0.125$.

To get a more accurate estimation, additional interference cancellation for pilot has been proposed at receiver, as shown in Fig. 5. The received signal will first pass through

TABLE 2: The weights of interference from different lattice points

-	n	$n+2$
$m-2$	-	$(-1)^{m-2}\beta$
$m-1$	-	$(-1)^{m-1}\gamma$
m	1	$(-1)^{m}\varepsilon$
$m+1$	-	$(-1)^{m+1}\gamma$
$m+2$	-	$(-1)^{m+2}\beta$

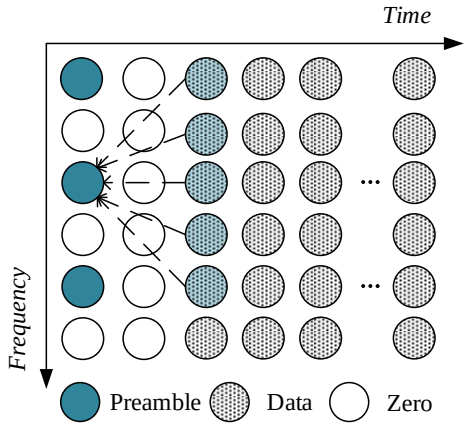

FIGURE 4: The data interference from surrounding symbols.

an FBMC demodulator. Then, after channel estimation and equalization, the demodulated data will be remodulated by an FBMC modulator just like the transmitter. It is worth noting that the data in the original pilot position will be set to zero. By passing through the estimated channel $\hat{\mathbf{H}}$, the data interference in the pilot position can be calculated. Finally, the data interference to the pilot is subtracted from the receiver. In the multi-stage configuration, the above processes are repeated until certain preset criteria is met. The specific signal processing flow in the receiver is described as follow.

After FBMC demodulation, the channel estimation $\hat{\mathbf{H}}$ can

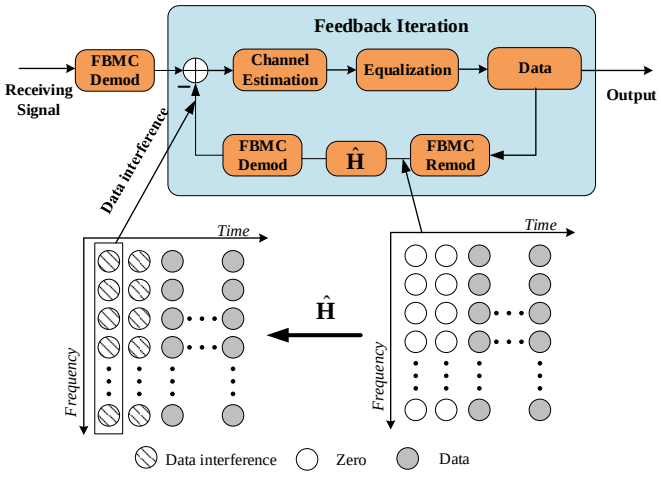

FIGURE 5: Proposed iterative receiver structure with feedback loops.

be calculated by extracting the pilot according to (25). Once the channel information is available, the received data can be equalized. The real part d_k^R and imaginary data part d_k^I of the k-th receiving antenna are expressed as

$$d_k^R = (\tilde{h}_k)^H r_k^R, d_k^I = (\tilde{h}_k)^H r_k^I \,, \tag{27}$$

where r_k^R and r_k^I represent the real and imaginary of r_k.

The next processes are similar to the transmitter, except that the pilot positions are all set to zeros. In order to match the receiving data, the signal has to pass through the channel and the demodulation at the receiver.

The feedback signal of one antenna can be expressed as

$$\tilde{r}(l) = \sum_{\tau=0}^{L_h-1} \tilde{h}(\tau) d_k(l-\tau) \,. \tag{28}$$

Therefore, the demodulation of feedback signal $\tilde{y}_{m,n}$ at the (m,n)-th time-frequency lattice point is given as

$$\tilde{y}_{m,n} = \hat{H}_{m,n}\tilde{a}_{m,n} + \sum_{(p,q)\neq(m,n)} \hat{H}_{p,q}\tilde{a}_{p,q}\zeta_{m,n}^{p,q}, \tag{29}$$

where $\tilde{a}_{m,n}$ represents the demodulated data at (m,n)-th lattice point in the receiver. The interference at the original pilot position is

$$\tilde{I}_{m,n} = \sum_{(p,q)\neq(m,n)} \hat{H}_{p,q}\tilde{a}_{p,q}\zeta_{m,n}^{p,q} \,. \tag{30}$$

Once the data interference is obtained, it will be subtracted from the receiver to get a more accurate channel estimation. Thus, the new received signal can be rewritten as

$$y_{m,n} = H_{m,n}a_{m,n} + \sum_{(p,q)\neq(m,n)} \left(\Delta\left(H_{p,q}a_{p,q}\right)\right)\zeta_{m,n}^{p,q} + \eta_{m,n}, \tag{31}$$

where $\Delta\left(H_{p,q}a_{p,q}\right) = H_{p,q}a_{p,q} - \hat{H}_{p,q}\tilde{a}_{p,q}$. As the number of feedbacks increases, the $\hat{H}_{p,q}$ is getting closer to $H_{p,q}$. In the limit case, $\Delta\left(H_{p,q}a_{p,q}\right)$ can be reduced to zero, resulting in an accurate channel estimate $\hat{\mathbf{H}}$.

Theoretically, in the multi-stage feedback configuration, as the number of iterations increases, more accurate channel estimation results are expected in high SNR region. The computational calculations in the feedback iteration loop and their computational complexities are shown in Table 3. After calculation, the computational complexity of the feedback loop is $O(MN \cdot {N_T}^4)$.

TABLE 3: Main mathematical computational complexities in the feedback loop

Mathematical operations	Size	Complexity
Matrix multiplication	$M_{n\times n}M_{n\times n}$	$O(n^3)$
Matrix multiplication	$M_{n\times m}M_{m\times n}$	$O(n\cdot m^2)$
Matrix inversion	$M_{n\times n}$	$O(n^3)$
FFT/IFFT	Length n	$O(n\log n)$
Loop computing function	n times	$O(n)$

V. SIMULATION RESULT

In this section, we will compare the spectrum efficiency of different systems and evaluate the performance of the proposed channel estimation method in terms of the estimation MSE and bit error rate (BER), respectively.

A. COMPARISON OF SPECTRUM EFFICIENCY

The normalized spectrum efficiency γ of MIMO-FBMC systems compared to ideal MIMO-OFDM systems with no overhead (i.e., no guard time interval and no frequency-domain training symbols) are

$$\begin{aligned}\gamma_{\text{FBMC}} &= \frac{N_D}{N_D+N_P} \times 100\% \\ \gamma_{\text{OFDM}} &= \frac{M}{N_{CP}+M} \times 100\%\end{aligned}, \tag{32}$$

where N_D and N_P denote the number of data and training symbols, and N_{CP} denotes the length of the cyclic prefix, respectively.

In a MIMO-OFDM system, with the utilization of CP, spectrum efficiency will suffer a certain degree of loss [40]. Even for LTE and 5G, the normalized spectrum efficiency reduces from 93.0% to 92.2% when the extended CP and normal CP change from 144 to 160 (among 2048 subcarriers). In contrast, a MIMO-FBMC system uses well-localized time-frequency pulse shaping filter to suppress the effect of dispersive channel, i.e., $N_{CP} = 0$. Both the IAM and ICM preamble require $N_T(G+1)$ real-valued symbols. Obviously, an increasing N_T will lower the spectrum efficiency of MIMO-FBMC systems.

The spectrum efficiency of CTSD has nothing to do with N_T, but it takes $3G+2$ real-valued training symbols. However, our proposed method only requires one real-valued training symbol (equivalent to half complex-valued symbol) and G zero symbols, even for a large number of transmit antennas. Because of this, our proposed channel estimation scheme owns higher spectrum efficiency, as shown in Table 4.

TABLE 4: Spectrum efficiency comparison ($N_D = 50$)

	MIMO-OFDM		MIMO-FBMC ($G=3$)		
	CP = 144	CP = 160	IAM&ICM	CTSD	Proposed
$N_T = 2$	93.0%	92.2%	92.6%	90.1%	96.2%
$N_T = 4$	93.0%	92.2%	86.2%	90.1%	96.2%
$N_T = 8$	93.0%	92.2%	75.8%	90.1%	96.2%

B. NUMERICAL SIMULATIONS FOR CHANNEL ESTIMATION PERFORMANCE

In this section, we evaluate the performance of the proposed real-valued orthogonal training sequences channel estimation with regard to the channel estimation MSE and BER. The corresponding simulation conditions are shown in Table 5.

The channel estimation MSE comparison (without feedback structure) is shown in Fig. 6 when $G = 1, 2, 3$. As can be seen, although the proposed new real-valued orthogonality sequences has reduced the training overhead, more interference (corresponding to larger estimation MSE values) has been introduced for $G = 1$ and $G = 2$. On the other hand, when $G = 3$, the estimation MSE of the proposed training scheme is very close to that of CTSD.

Fig. 7 shows the MSE performance of the proposed feedback structure with different guard intervals ($G = 1, 2, 3$)

TABLE 5: MIMO-FBMC system channel estimation simulation parameters

Subcarrier Number	256
Prototype Filter	PHYDYAS, $K = 4$
Signal Modulation Mode	QPSK
Channel	Multipath with equal power taps
Multipath Number	$L_h = \{3, 6, 9\}$
Guard Interval	$G = \{1, 2, 3\}$
Antenna Number	$N_T = 4$

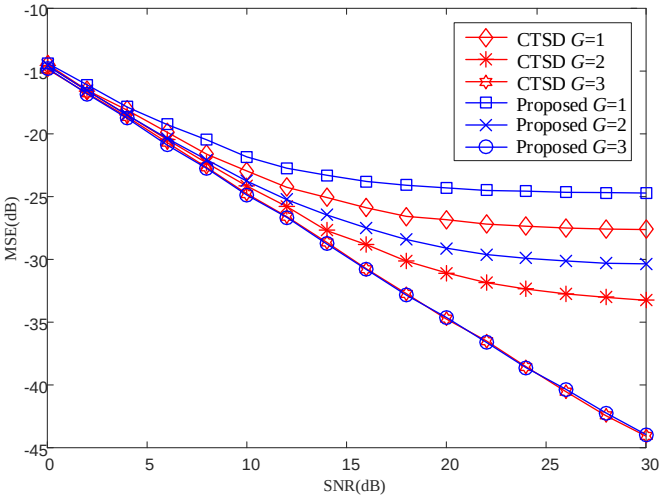

FIGURE 6: MSE performance comparison between CTSD and the proposed method (without feedback structure).

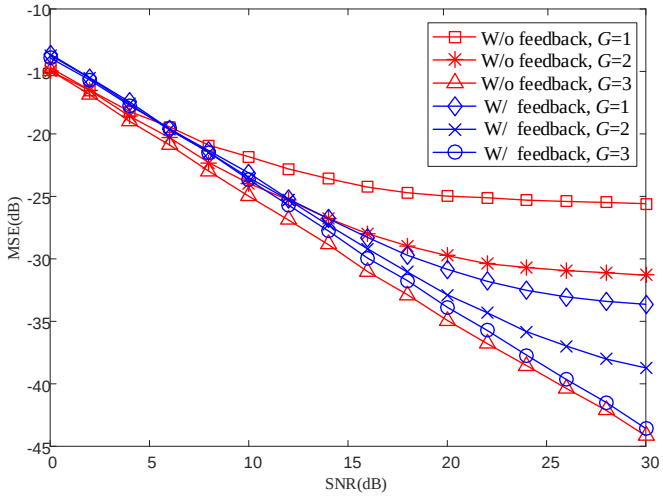

FIGURE 7: MSE performance comparison with feedback structure.

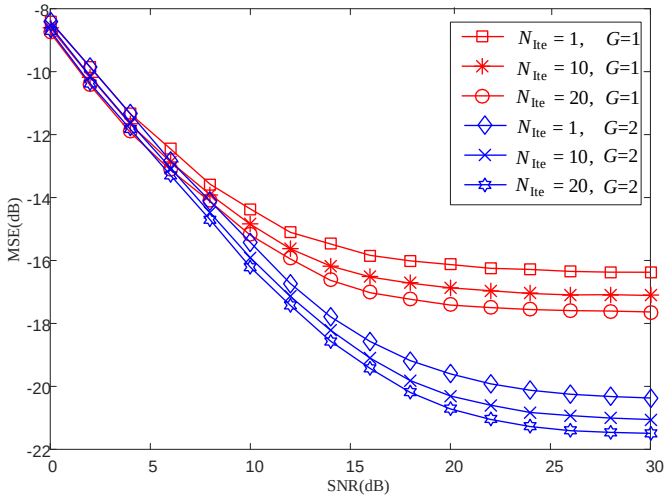

FIGURE 8: MSE performance comparison in present of feedback loops in EVA channel.

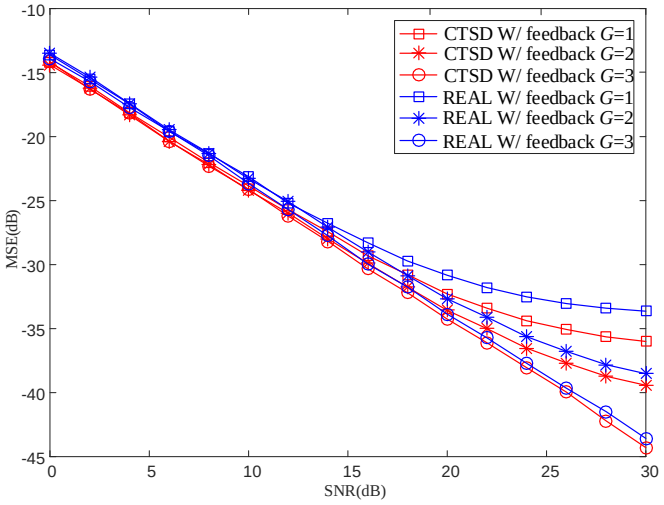

FIGURE 10: Performance comparison of CTSD and real-valued method with feedback structure.

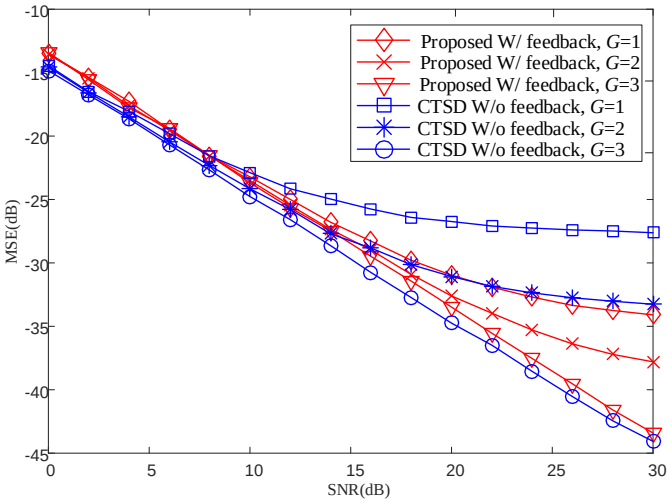

FIGURE 9: MSE performance comparison of our proposed method and CTSD for MIMO-FBMC systems.

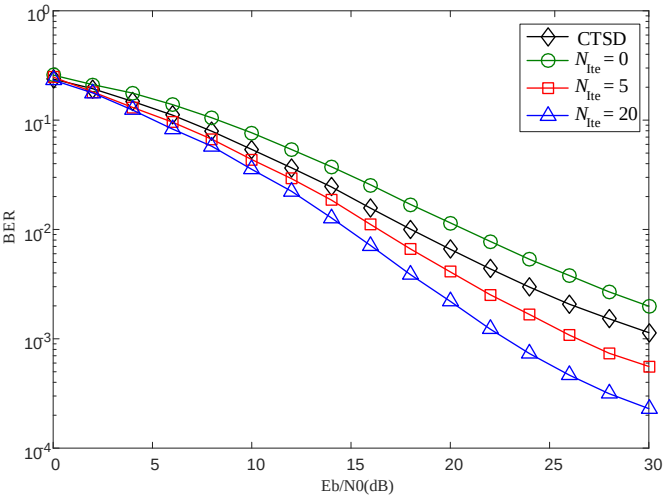

FIGURE 11: BER performance comparison of our feedback iteration method (different iteration times) with CTSD when $L_h = 6, G = 2$.

in multipath channel. One can see that significant MSE performance improvement is achieved in high SNR region when $G = 1, 2$. Due to the error propagation, the proposed channel estimation method with feedback performs worse when the SNR is small (e.g., below 5 dB).

Fig. 8 shows the MSE performance in an EVA channel. Extended Vehicular A model is a typical multipath channel and often used for related communication system simulation [41]. Each path of the EVA model has different delay and power. As the number of feedback iterations increases, the estimation MSE gets improved, although the improvement becomes smaller for larger value of iteration number. Hence, in practical system design, 10 or less iterations is suggested.

Fig. 9 compares our proposed channel estimation (5 times of iteration) with the CTSD scheme. For a fair comparison, the average power of the training sequences (preamble symbol and the guard interval) is set to be identical. Simulation result shows that the proposed method leads to improved MSE (compared with CTSD) for $G = 1, 2$. This is because the data interference is largely eliminated through feedback and multiple iterations.

To illustrate the generality of the feedback structure, this structure is also applied to CTSD. Fig. 10 shows the MSE performance comparison of CTSD and the proposed training sequences which are both based on feedback iterative structure. Compared with Fig. 6 and Fig. 9, as can be seen, the performance of CTSD has been greatly improved with the aid of feedback structure. This demonstrates the effectiveness and generality of the proposed feedback iteration structure in the field of channel estimation.

Lastly, Fig. 11 shows the BER performance comparison of the proposed feedback iteration method with CTSD when

$L_h = 6$ and $G = 2$. It is shown that the BER performance is worse than CTSD when $N_{Ite} = 0$ (without feedback iteration). But as the iteration number increases, our proposed channel estimation method leads to the enhanced BER.

VI. CONCLUSION

In this paper, we have proposed a real-valued orthogonality sequence set for efficient training symbols over one OQAM symbol duration in MIMO-FBMC systems. This improves the training efficiency of our previous CTSD approach [23] which requires two OQAM symbols. In addition, an interference cancellation based on feedback structure has been developed. We have shown that the inherent interference can be substantially eliminated and hence improved channel estimation can be obtained. Simulation results show that our proposed real-valued orthogonal sequences and feedback iteration method can improve both the channel estimation and error rate performances in MIMO-FBMC systems.

REFERENCES

[1] B. Hirosaki, "An orthogonally multiplexed QAM system using the discrete Fourier transform," *IEEE Trans. Commun.*, vol. 29, no. 7, pp. 982-989, 1981.
[2] B. Le Floch, M. Alard and C. Berrrou, "Coded orthogonal frequency division multiplex," *Processings of the IEEE*, vol. 83, no. 6, pp, 982-996, 1995.
[3] X. Gao, W. Wang, X. Xia, E. K. S. Au and X. You "Cyclic prefixed OQAM-OFDM and its application to single-carrier FDMA," *IEEE Trans. Commun.*, vol. 59, no. 5, pp. 1467-1480, 2011.
[4] J.-P. Javaudin, D. Lacroix and A. Rouxel, "Pilot-aided channel estimation for OFDM/OQAM," *The 57th IEEE Semiannual Vehicular Technology Conference*, vol. 3, pp. 1581-1585, 2003.
[5] P. Siohan, C. Siclet and N. Lacaille, "Analysis and design of OQAM-OFDM systems based on filterbank theory," *IEEE Trans. Signal Process.*, vol. 50, no. 5, pp. 1170-1183, 2002.
[6] J. Du, "Pulse shape adaptation and channel estimation in generalized frequency division multiplexing systems," *Licentiate Thesis, KTH*, 2008.
[7] C. Lele, J.-P. Javaudin, R. Legouable, A. Skrzypczak and P. Siohan, "Channel estimation methods for preamble-based OFDM/OQAM modulations," *Proc. Eurpean Wireless Conf.*, pp. 59-64, 2007.
[8] C. Lele, P. Siohan and R. Legouable, "2dB better than CP-OFDM with OFDM/OQAM for preamble-based channel estimation," *Proc. of Int. Conf. Commun.*, pp. 1302-1306, 2008.
[9] J. Du and S. Signell, "Novel preamble-based channel estimation for OFDM/OQAM systems," *Proc. of Int. Conf. Commun.*, pp. 14-18, 2008.
[10] S. W. Kang, K. H. Chang, "A novel channel estimation scheme for OFDM/OQAM-IOTA system," *ETRI Journal*, vol. 29, no. 4, pp. 430-436, 2007.
[11] S. Hu, G. Wu, T. Li, Y. Xiao and S. Li, "Preamble design with ICI cancellation for channel estimation in OFDM/OQAM system," *IEICE Trans. Commun*, E93-B, pp. 211-214, 2010.
[12] D. Kong, D. Qu and T. Jiang, "Time domain channel estimation for OQAM-OFDM systems: algorithms and performance bounds," *IEEE Trans. Signal Process.*, vol. 62, no. 2, pp. 322-330, 2014.
[13] AI. Perez-Neira, M. Caus, R. Zakaria *et al*, " MIMO signal processing in offset-QAM based filter bank multicarrier systems," *IEEE Trans. Signal Process.*, vol. 64, no. 21, pp. 5733-5762, 2016.
[14] E. Kofidis,"Preamble-based estimation of highly frequency selective channels in FBMC/OQAM systems," *IEEE Transactions on Signal Processing*, vol. 65, no. 7, pp.1855-1868, 2017.
[15] E. Kofidis and D. Katselis, "Preamble-based channel estimation in MIMO-OFDM/OQAM systems," *Proc. IEEE Int. Conf. Signal Image Process. Appl.*, pp. 579-584, 2011.
[16] E. Kofidis, "Preamble-based estimation of highly frequency selective channels in MIMO-FBMC/OQAM systems," *Proc. 21th Eur. Wireless Conf.*, Budapest, Hungary, pp. 1-6, 2015.
[17] S. Taheri, M. Ghoraishi and P. Xiao, "Overhead reduced preamble-based channel estimation for MIMO-FBMC systems," *Proc. Int. Wireless Commun. Mobile Comput. Conf.*, pp. 1435-1439, 2015.
[18] Z. Na, Y. Wang, X. Li *et al*, "Subcarrier allocation based Simultaneous Wireless Information and Power Transfer algorithm in 5G cooperative OFDM communication systems," *Physical Communication*, vol. 29, pp. 164-170, 2018.
[19] S. A. Yang, J. Wu, "Optimal binary training sequence design for multiple-antenna systems over dispersive fading channels," *IEEE Trans. Veh. Technol.*, vol. 51, no. 5, pp. 1271-1276, 2002.
[20] P. Fan and W. H. Mow, "On optimal training sequence design for multiple-antenna systems over dispersive fading channels and its extensions," *IEEE Trans. Veh. Technol.*, vol. 53, no. 5, pp. 1623-1626, 2004.
[21] S. He, Y. Huang, S. Jin and L. Yang, "Coordinated beamforming for energy efficient transmission in multicell multiuser systems," *IEEE Trans. Commun.*, vol. 61, no. 12, pp. 4961-4971, 2013.
[22] C. Fragouli, N. Al-Dhahir and W. Turin, "Training-based channel estimation for multiple-antenna broadband transmissions," *IEEE Trans. Wireless Commun.*, vol. 2, no. 2, pp. 384-391, 2003.
[23] S. Hu, Z. Liu, Y. Guan *et al*, "Training sequence design for efficient channel estimation in MIMO-FBMC systems," *IEEE Access*, vol. 5, pp. 4747-4758, 2017.
[24] Z. Na, J. Lv, M. Zhang *et al*, "GFDM Based Wireless Powered Communication for Cooperative Relay System," *IEEE Access*, vol. 7, pp. 50971-50979, 2019.
[25] X. Tang, P. Fan and S. Matsufuji, "Lower bounds on the maximum correlation of sequence set with low or zero correlation zone," *Electron. Lett.*, vol. 36, no. 6, pp. 551-552, 2000.
[26] H. Torii, M. Nakamura and N. Suehiro, "A new class of zero-correlation zone sequences," *IEEE Trans. Inf. Theory*, vol. 50, no. 3, pp. 559-565, 2004.
[27] X. Tang, P. Fan, D. Li and N. Suehiro, "Binary array set with zero correlation zone," *IEE Electron. lett.*, vol. 37, pp. 841-842, 2001.
[28] A. Rathinakumar and A. K. Chaturvedi, "A new framework for constructing mutually orthogonal complementary sets and ZCZ sequences," *IEEE Trans. Inf. Theory*, vol. 52, pp. 3817-3826, 2006.
[29] S. Hu, Z. Liu, Y. L. Guan, W. Xiong, G. Bi and S. Li, "Sequence design for cognitive CDMA communications under arbitrary spectrum hole constraint," *IEEE J. Sel. Areas Commun.*, vol. 32, no. 11, pp. 1974-1986, 2014.
[30] M. Jia, Z. Yin, Q. Guo, G. Liu and X. Gu, "Downlink design for spectrum efficient IoT network," *IEEE IOTJ*, vol. 5 , no. 5, pp. 3397 - 3404, 2018.
[31] M. Jia, X. Gu, Q. Guo, W. Xie and N. Zhang, "Broadband hybrid satellite-terrestrial communication systems based on cognitive radio toward 5G," *IEEE Wireless Commun.*, vol. 23 , no. 6, pp. 96-106, 2016.
[32] S. Hu, B. Yu, C. Qian, Y. Xiao, Q. Xiong, C. Sun and Y. Gao, "Non-orthogonal interleave-grid multiple access scheme for industrial internet of things in 5G network," *IEEE Trans. Ind. Inform.*, vol. 14 , no. 2, pp. 5436-5446, 2018.
[33] S. Hu, G. Bi, Y. L. Guan, and S. Li, "TDCS-based cognitive radio networks with multiuser interference avoidance," *IEEE Trans. Commun.*, vol. 61 , no. 12, pp. 4828-4835, 2013.
[34] X. Liu, M. Jia, and Z. Na, "Multi-modal cooperative spectrum sensing based on dempster-shafer fusion in 5G-based cognitive radio," *IEEE ACCESS.*, vol. 6, pp. 199-208, 2018.
[35] X. Liu, X. Zhang, M. Jia, "5G-based green broadband communication system design with simultaneous wireless information and power transfer," *Physical Communication*, vol. 25, pp. 539-545, 2018.
[36] E. Kofidis, D. Katselis, A. Rontogiannis and S. Theogoridi, "Preamble-based channel estimation in OFDM/OQAM systems: A review," *Signal Process.*, vol. 93, no. 7, pp. 2038-2054, 2013.
[37] PHYDYAS European project, http://www.ict-phydyas.org.
[38] J. Du, S. Signell, "Time frequency localization of pulse shaping filters in OFDM/OQAM systems," *Proc. of Int. Conf. Commun.* pp.1-5, 2007.
[39] H. Bolcskei, H. G. Feichtinger and T. Strohmer, "Orthogonal frequency divison multiplexing based on offset OQAM," *Advances in Gabor Analysis*, pp. 321-352, 2003.
[40] W. Lu, S. Fang, S. Hu *et al*, "Energy efficiency optimization for OFDM based 5G wireless networks with simultaneous wireless information and power transfer," *IEEE ACCESS*, vol. 6, pp. 75937-75946, 2018.
[41] H. Qu, G. Liu, Y. Wang *et al*, "Time-Domain Channel Estimation for the LTE-V System Over High-Speed Mobile Channels," *2018 IEEE International Symposium on Broadband Multimedia Systems and Broadcasting (BMSB)*, 2155-5052, Jun. 2018.